SIAM J. APPL. MATH.
Vol. 39, No. 1, August 1980

0036-1399/80/3901-0012 $01.00/0

BOUNDARY EFFECTS IN NEURAL NETWORKS*

LAWRENCE SIROVICH†

Abstract. The boundary of a neural network is considered, and the Hartline–Ratliff equations are used as a model system. Solutions are obtained by means of the Wiener–Hopf technique. Specific examples are calculated and comparison with experiment is made.

1. Introduction. It is the purpose of this paper to consider the effect of a boundary on the workings of a neural network. We will in particular apply our treatment to the case of the lateral eye of the horseshoe crab, *Limulus*.

Neural response, which we denote by r, in most cases is expressed as impulses per time. It represents the rate at which a neuron generates action potentials in response to a stimulus, s. In addition to the stimulus, the response activity in the neighborhood of a neuron mediates its impulse rate. Symbolically we can write this as

$$r(\mathbf{x}, t) = M(s) - N(r), \tag{1}$$

where M and N are in general operators in time and space. A negative sign appears in (1) to underline the fact that neural activity for the most part occurs as an antagonistic interaction between excitation and inhibition. In this way a neutral network sharpens features and in other ways abstracts information.

A network described by (1) is said to be of recurrent type. It has the property that two neurons may affect one another in the absence of a direct connection if there is some sequence of connections between them. Thus, for example, a point stimulus can spread its influence throughout a recurrent network, in contrast to a nonrecurrent network, $N = 0$, where a point stimulus only affects directly connected parts of the network.

With one exception, the operators N and M have substantial linear operating ranges. The exception pertains to the fact that a neuron can only fire impulses at a positive rate. Thus there is a threshold effect. This threshold, which may be greater than zero, is denoted by r_0. With these assumptions (1) becomes

$$r = Ms - N\theta(r - r_0), \tag{2}$$

where θ is the positive part operator,

$$\theta(x) = \tfrac{1}{2}(x + |x|) \tag{3}$$

and N and M are now taken to be linear spatio-temporal operators. (It is clear that the right-hand side of (2) should also be replaced by $\theta(Ms - N\theta(r - r_0))$; however, as a little thought reveals, taking the positive part of the solution to (2) yields the same result.)

Another feature common to many neural networks is that they show a high degree of homogeneity. Slow departures from homogeneity can occur in the network, but we approximate by homogeneity. We add in passing that a repetitive network or one with a high degree of symmetry is easier to construct (i.e., easier to code for development) and in addition provides a likely mechanism for parallel processing. This in turn allows a nervous system to extract information from an ensemble of noisy signals. For the case of the lateral eye of *Limulus*, a number of physiological investigations support the

* Received by the editors March 6, 1979.

† Division of Applied Mathematics, Brown University, Providence, Rhode Island 02912 and Rockefeller University, New York, New York 10021. This research was supported in part by the National Science Foundation under Grant MCS 77-08598, and by the United States Eye Institute under Grants EY 188, EY 1428, EY 1472.

hypothesis of homogeneity (Barlow [1]; Brodie, Knight, Ratliff [2], [3]; Sirovich, Brodie, Knight [4]).

With reference to (2), it is to be expected that both M and N, within reasonable time scales, are time stationary operators. From homogeneity in space and stationarity in time it follows that (2) can be written in the form

$$r(\mathbf{x}, t) = \int_{-\infty}^{t} d\tau \int M(t-\tau, \mathbf{x}-\mathbf{y}) s(\mathbf{y}, \tau)\, d\mathbf{y} - \int_{-\infty}^{t} d\tau \int N(t-\tau, \mathbf{x}-\mathbf{y}) \theta[r(\mathbf{y}, \tau) - r_0]\, d\mathbf{y}. \tag{4}$$

The upper limit of t in the temporal integration follows from causality.

From the form in which M occurs, it may be suppressed, i.e., $M(s)$ itself can be regarded as the effective stimulus. This brings up an interesting distinction between theory and experiment. In experiment one supplies the data, s, and in effect measures the solution r. The goal then is to determine M and N, or rather highly factored forms of these which then reveal component transductions. Aside from general restrictions, such as causality, stationarity, homogeneity and symmetry, which we have used, there are no obvious basic forms for these operators. Because this is a theoretical study we regard M and N as known operators, already arrived at from experiment.

The present study deals with the boundary of a neural network and therefore considers the effect of a sharp inhomogeneity. As a working hypothesis we assume that a boundary network is a truncated form of the interior network. Support for this view comes from a related experimental investigation [4].

2. Hartline–Ratliff equations. The common horseshoe crab, *Limulus*, has a compound eye, composed of roughly one thousand photoreceptors or ommatidia. These ommatidia are coupled to one another by an inhibitory network in the eye. Individual photoreceptor responses, measured by electrophysiological means, have been well-modeled by the Hartline–Ratliff equations (Hartline and Ratliff [5]; Knight et al. [6]). (For extensions see Lange [7], Barlow and Lange [8], and Barlow and Quarles [9].) The continuous version of these equations (Kirschfeld and Reichardt [10]) have proven their usefulness in the laboratory [2], [3] and will be employed here. Equations (1), (2), and (4) each represent a generalized form of the continuous Hartline–Ratliff equations.

The workings of the *Limulus* eye may be represented in terms of a block diagram (Dodge [11]). A simplified version of this is shown in Fig. 1. The stimulus is an

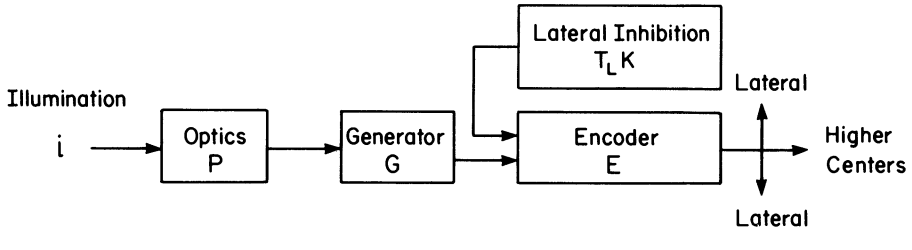

FIG. 1. *Block diagram for the* Limulus *lateral eye. The illumination pattern falling on the eye is denoted by i. The optics of the eye (and possibly the experimental apparatus) is denoted by P. The incident light is transduced into an intracellular potential GPi which in turn is encoded into an impulse train, EGPi. This signal passes on to higher centers and simultaneously travels laterally to inhibit neighboring photoreceptor outputs. The last transduction is controlled by the product operator $T_L K$; in which K is spatial and T_L temporal.*

illumination pattern and we denote it by $i(\mathbf{x}, t)$. This light passes through optics, P, before falling on the retina. It produces, at each photoreceptor location, an intracellular voltage, GPi, known as the generator potential. This in turn is transduced into a train of nerve impulses by the encoder mechanism, denoted by E. Both E and G are linear operators in the time domain, while P, the linespread function of the optics, is a linear spatial operator. The output at a location, i.e., the response, denoted by r, travels to higher centers and in addition passes laterally to nearby locations and inhibits the response activity there. In the same way nearby response inhibits the response at the point in question by summing negatively with the generator potential. This lateral effect has a product form, $T_L\hat{K}$, where T_L is temporal and $\hat{K}$ is spatial (Ratliff et al. [12]). The threshold, r_0, for lateral inhibition, will be taken to be a constant, which from [9] we can suppose lies close to zero.

From this discussion and Fig. 1, we can write instead of (2),

$$r = E(GPi - T_L\hat{K}\theta(r - r_0)), \tag{5}$$

and instead of (4)

$$r = \int_{-\infty}^{t} E(t-\tau)\, d\tau \Big\{ \int_{-\infty}^{\tau} G(\tau-\mu) \int d\mathbf{y}\, P(\mathbf{x}-\mathbf{y}) i(\mathbf{y}, \mu)\, d\mu - \int_{-\infty}^{\tau} T_L(\tau-\mu)\, d\mu \int \hat{K}(\mathbf{x}-\mathbf{y})\theta(r(\mathbf{y}', \mu) - r_0)\, d\mathbf{y} \Big\}. \tag{6}$$

As a result of the brevity of the above exposition a number of important details have been overlooked. Notable among the omissions is the decomposition of the encoding operator, E, and discussion of the optical properties of the crab eye, [3]. A discussion of these and other properties can be found in (Ratliff [13]).

Normalization. The impulse rate can be normalized by setting

$$\rho = \frac{r - r_0}{r^0},$$

where r^0 is a constant, representative of the recorded impulse rate. Also define the total inhibition as

$$K_0 = \int_{-\infty}^{\infty} \hat{K}(\mathbf{x})\, d\mathbf{x},$$

normalize the kernel by

$$K = \hat{K}/K_0,$$

and set

$$S = K_0 E T_L. \tag{7}$$

It then follows that (5) may be written as

$$\rho = e - SK\theta(\rho), \tag{8}$$

where

$$e = (EGPi - r_0)/r^0, \tag{9}$$

which we term the equivalent stimulus.

If we restrict attention to cases for which $\rho \geqq 0$ and consider one-dimensional patterns, $i(x, t)$ (which implies $\rho = \rho(x, t)$) then (6) becomes

$$\rho = e(x, t) - \int_{-\infty}^{t} S(t-\tau) \int_{-\infty}^{\infty} K(x-x')\rho(x', \tau)\, dx'\, d\tau. \tag{10}$$

Transforms. In order to discuss further properties it is convenient to introduce the Fourier transform in time

$$\int_{-\infty}^{\infty} \rho(x, t) \exp(-i\omega t)\, dt = \rho(x, \omega), \tag{11}$$

and the Fourier transform in space

$$\int_{-\infty}^{\infty} \rho(x, t) \exp(-i\xi x)\, dx = \rho(\xi, t). \tag{12}$$

Note that we use the same symbol for transformed variables, since the arguments of a function indicate the nature of the transform. If we apply (11) and (12) to (10) we obtain

$$\rho(\xi, \omega) = e(\xi, \omega) - S(\omega)K(\xi)\rho(\xi, \omega). \tag{13}$$

For a purely temporal pattern $e = e(t)$, (13) becomes

$$\rho(\omega) = e(\omega) - S(\omega)\rho(\omega)$$

or

$$\rho(\omega) = \frac{e(\omega)}{1+S(\omega)}, \tag{14}$$

the solution of which is

$$\rho(t) = \frac{1}{2\pi} \int_{-\infty}^{\infty} \frac{e(\omega)}{1+S(\omega)} \exp[i\omega t]\, d\omega. \tag{15}$$

Properties of S. The transform of S is

$$\begin{aligned} S(\omega) &= \int_0^{\infty} \exp(-i\omega t)S(t)\, dt = K_0 \int_0^{\infty} \exp(-i\omega t)T_L(t)\, dt \int_0^{\infty} \exp(-i\omega t')E(t')\, dt' \\ &= K_0 E(\omega) T_L(\omega). \end{aligned} \tag{16}$$

That these integrals extend over the half-line $(0, \infty)$ is a consequence of causality. Further because (15) must also behave in a causal manner, we have that

$$1 + S(\omega) \neq 0, \qquad \operatorname{Im} \omega < 0. \tag{17}$$

[Alternatively if a Laplace instead of a Fourier transform is used, condition (17) guarantees a solution stable in time.] Also from (16) $S(\omega)$ and hence $1 + S(\omega)$ is analytic for $\operatorname{Im} \omega < 0$.

Properties of K. In addition to the property of homogeneity or translational invariance, K can be assumed to be symmetric [2],

$$K(x) = K(-x).$$

The actual form of $K(x)$ follows from laboratory measurements (Barlow [1], [14], Kirschfeld and Reichardt [10], Johnston and Wachtel [15]). In [2] it is represented by a difference of Gaussians. On the other hand, the same data can be equally well-

represented by a sum of 'back-to-back' exponentials, say

$$K(x) \approx \sum_n \alpha_n \exp(-\beta_n |x|).$$

This is shown to be the case in [4]. It therefore follows that

$$K(\xi) = \frac{N(\xi^2)}{D(\xi^2)}, \tag{18}$$

where N and D are real polynomials such that

$$\deg N < \deg D.$$

Actually in assuming (18) we consider a class which also includes damped sinusoidal variation in $K(x)$.

Next, from experiment we postulate that (9) does not possess free running wave solutions. This means that $\exp(i\omega t + i\xi x)$ for real ω and ξ cannot be a solution of the homogeneous form of (9), or that

$$D(\xi^2) + S(\omega)N(\xi^2) \neq 0, \quad \text{for } \omega \text{ and } \xi \text{ real.} \tag{19}$$

3. The transfer function. In practice, the ratio $\rho(\xi, \omega)/e(\xi, \omega)$, is known as a transfer function. In terms of (13) this transfer function is given by

$$\frac{\rho(\xi, \omega)}{e(\xi, \omega)} = p(\xi, \omega) = \frac{1}{1 + S(\omega)K(\xi)}. \tag{20}$$

In terms of the operators in (6), we obtain the transfer function as it is customarily measured in the laboratory

$$\mathcal{F}(\xi, \omega) = \frac{G(\omega)E(\omega)P(\xi)}{1 + E(\omega)T_L(\omega)K(\xi)}.$$

Properties of the component operators can be extracted from a study of the transfer function itself [2], [3]. The transfer function, (20), also may be interpreted as the transform of the fundamental solution, i.e. the solution with a delta function stimulus, $e = \delta(t)\delta(x)$.

In the present context we are interested in the form taken by (19) under the assumption (18). In this case

$$p(\xi, \omega) = \frac{D(\xi^2)}{D(\xi^2) + S(\omega)N(\xi^2)}. \tag{21}$$

To factor D we denote its degree by $2M$ and write

$$D(\xi^2) = \prod_{n=1}^{M} (\xi^2 - \xi_n^2). \tag{22}$$

As a consequence of (18),

$$\operatorname{Im}(\xi_n) \neq 0,$$

and to fix the choice of the roots we take

$$\operatorname{Im} \xi_n > 0. \tag{23}$$

Likewise we can factor the denominator of (21) into the form

$$D(\xi^2) + S(\omega)N(\xi^2) = \prod_{n=1}^{M} (\xi^2 - \lambda_n^2(\omega)). \tag{24}$$

As in the above we can fix $\lambda_n(\omega)$ by the condition

$$\text{Im } \lambda_n(\omega) > 0. \tag{25}$$

This follows from (19) which in effect states that $\lambda_n(\omega)$ cannot cross the real axis, for real ω.

Next we consider the branch structure of (24). To this end we locate the critical or branch points by considering the simultaneous solution of

$$\begin{aligned} &D(\xi^2)+S(\omega)N(\xi^2)=0, \\ &\frac{\partial}{\partial \xi}(D(\xi^2)+S(\omega)N(\xi^2))=2\xi(D'(\xi^2)+S(\omega)N'(\xi^2))=0. \end{aligned} \tag{26}$$

(We may assume that (24) is irreducible.)

Two different cases arise depending on whether the root, ξ, of (26) is or is not zero.

Case 1. Root: $\xi = 0$. In this case

$$D(0)+S(\omega)N(0)=0=1+S(\omega). \tag{27}$$

It follows from (17) that no branch points lie in the lower half-plane. Of course $\lambda_n(\omega)$ can have branch points of $S(\omega)$ itself, but these must lie in the upper half plane.

Case 2. Root not zero; $\xi \neq 0$. In this case set $w = \xi^2$ and suppress the dependence of S on ω. Thus instead of (26) we consider

$$\begin{aligned} &D(w)+SN(w)=\prod_{n=1}^{M}(w-w_n(S))=0, \\ &D'(w)+SN'(w)=0. \end{aligned} \tag{28}$$

If we eliminate S, then

$$\frac{D'(w)}{D(w)}+\frac{N'(w)}{N(w)}=0,$$

and if we eliminate w we obtain the discriminant which we denote by

$$\Delta(S)=0. \tag{29}$$

When S^0 is a solution to this equation it can be a branch point of $w_n(S)$. If S loops S^0 in the complex S-plane the collection of roots $(w_1(S), w_2(S), \cdots, w_M(S))$ are permuted. Thus any symmetrical function of these roots does not have S^0 as a branch point since it returns to its original value under the looping. As a trivial example

$$D(w)+SN(w)=\prod_{n=1}^{M}(\xi^2-\lambda_n^2)$$

has no roots of (29) as branch points other than those that $S(\omega)$ may have. As another example

$$\prod_{n=1}^{M}(\xi+\sqrt{w_n(S)})=\prod_{n=1}^{M}(\xi+\lambda_n(\omega)) \tag{30}$$

has no root of (29) as a branch point. It can, however, have the branch points found for Case 1, namely those for which a $w_n = 0$.

As a result of the above factorization we can write the transfer function in the form

$$p(\xi,\omega)=\prod_{n=1}^{M}\frac{\xi^2-\xi_n^2}{\xi^2-\lambda_n^2(\omega)}. \tag{31}$$

4. Drifting patterns. In a laboratory situation, solutions to (8) can be made to conform to its linear range (so that (10) is appropriate) by imposing a uniform background illumination. Thus if e_0 is a constant it leads to the solution

$$\rho_0 = \frac{e_0}{1+S_0}. \tag{32}$$

In speaking of solutions to (10) we will assume that a sufficiently high background is present so that if ρ becomes negative it does not indicate an inconsistency but rather that $\rho+\rho_0$ is positive, and (10) is still appropriate. Knight [16], introduced uniformly drifting patterns of illumination and in [2], [3] such patterns are considered in more detail. A stimulus pattern is drifted across the eye with a constant speed, i.e.

$$e(x, t) = e(x+Vt) = \tilde{e}\left(t+\frac{x}{V}\right). \tag{33}$$

The solution to (10) can then be assumed to take the same form,

$$\rho = \rho(x+Vt). \tag{34}$$

If (33) and (34) are substituted into (5) the solution is easily obtained by means of spatial transform

$$\rho(x+Vt) = \frac{1}{2\pi}\int_{-\infty}^{\infty} \frac{e(\xi)\exp[i\xi(x+Vt)]}{1+S(\xi V)K(\xi)}\,d\xi. \tag{35}$$

Alternatively, through use of the last form of (33), this may be represented as a temporal inversion

$$\rho(x+Vt) = \frac{1}{2\pi}\int_{-\infty}^{\infty} \frac{\exp[i\omega(t+(x/V)]}{1+S(\omega)K(\omega/V)}\,\tilde{e}(\omega)\,d\omega. \tag{36}$$

If we return to the form for the transfer function (31), then

$$p_f(\omega) = p\left(\frac{\omega}{V}, \omega\right) = \frac{\prod_{n=1}^{M}((\omega^2/V^2)-\xi_n^2)}{\prod_{n=1}^{M}((\omega^2/V^2)-\lambda_n^2(\omega))} \tag{37}$$

is the temporal transform of the fundamental solution i.e., when $e = \delta(x+Vt)$. In fact

$$\rho(0, t) = p_f(t) * \tilde{e}(t) \tag{38}$$

is the solution at the origin and

$$\rho(x, t) = p_f\left(t+\frac{x}{V}\right) * \tilde{e}(t) \tag{39}$$

is the solution everywhere.

5. The edge problem. The problem of physical interest to us is that of the response in the neighborhood of the boundary of the eye. In the experimental situation this is replaced by a simulated boundary, namely a shadow edge [4]. The eye to the left of $x=0$ is maintained in darkness, while for $x>0$ a background and a drifting pattern is imposed. If we return to (6) we see that the appropriate form of the equation is now

$$\rho(x, t) = e(x, t) - \int_{-\infty}^{t} S(t-\tau)\,d\tau \int_0^{\infty} K(x-y)\rho(y, \tau)\,dy$$

where the stimulus is composed of a background $e^0H(x)$ ($H(x)$ is the Heaviside

function) plus a drifting pattern. It will suffice if we consider e to be of the form $e(x+Vt)$, in which case we can set $V=0$ and take $e(x)=e^0H(x)$ to solve for the background response. Unlike the full eye case where the background solution is a constant, (32), the steady state is now nontrivial.

We therefore consider

$$\rho(x,t)=e(x+Vt)-\int_{-\infty}^{t} S(t-\tau)\,d\tau\int_0^{\infty} K(x-y)\rho(y,\tau)\,dy. \tag{40}$$

Under Fourier transformation in time this becomes

$$\rho(x,\omega)=\tilde{e}(\omega)\exp[i\omega x/V]-S(\omega)\int_0^{\infty} K(x-y)\rho(y,\omega)\,dy.$$

Instead of ρ we seek the fundamental solution, $p(x,t)$ which is defined by

$$\rho(x,\omega)=\tilde{e}(\omega)p(x,\omega). \tag{41}$$

Clearly

$$\rho(x,t)=p*\tilde{e}(t), \tag{42}$$

where the convolution is in the time domain.

Under the substitution (41) we obtain

$$p(x,\omega)=\exp\left[\frac{i\omega x}{V}\right]-S(\omega)\int_0^{\infty} K(x-y)p(y,\omega)\,dy. \tag{43}$$

Wiener–Hopf technique. We propose to solve (43) by the Wiener–Hopf technique (Noble [17]). To this end we define

$$\sigma(x,\omega)=\begin{cases}-\exp\left[\dfrac{i\omega x}{V}\right]+S(\omega)\displaystyle\int_0^{\infty} K(x-y)p(y,\omega)\,dy, & x<0,\\ 0, & x>0.\end{cases}$$

and $p(x,\omega)=0$, $x<0$. Instead of (43) we obtain

$$p(x,\omega)=\exp\left[\frac{i\omega z}{V}\right]+\sigma(x,\omega)-S(\omega)\int_{-\infty}^{\infty} K(x-y)p(y,\omega)\,dy. \tag{44}$$

If we Fourier transform (44) we obtain

$$p^-(\xi,\omega)=2\pi\delta\left(\xi-\frac{\omega}{V}\right)+\sigma^+(\xi,\omega)-S(\omega)K(\xi)p^-(\xi,\omega), \tag{45}$$

where

$$p^-(\xi,\omega)=\int_0^{\infty}\exp[-i\xi x]p(x,\omega)\,dx \tag{46}$$

is analytic in the lower half-plane and

$$\sigma^+(\xi,\omega)=\int_{-\infty}^{0}\exp[-i\xi x]\sigma(x,\omega)\,dx$$

is analytic in the upper half-plane. δ in (45), which represents the "delta function," may be represented by

$$\delta\left(\xi-\frac{\omega}{V}\right)=\frac{1}{2\pi i}\left(\frac{1}{\xi-(\omega/V)-i\varepsilon}-\frac{1}{\xi-(\omega/V)+i\varepsilon}\right), \tag{47}$$

where $\varepsilon > 0$ is a vanishingly small quantity. For later purposes we observe, if $p(x, \omega)$ has an integrable derivative, then by parts integration of (46),

$$p^-(\xi, \omega) = \frac{p_e(\omega)}{i\xi} + o\left(\frac{1}{\xi}\right), \tag{48}$$

where $p_e(\omega) = p(x = 0, \omega)$ is the transform of the response at the edge. The error estimate follows from the Riemann–Lebesgue lemma, [18].

Next we substitute (47) and (31) into (45), which after some rearrangement is

$$\begin{aligned} p^-(\xi, \omega) \prod_{n=1}^{M} \left(\frac{\xi^2 - \lambda_n^2(\omega)}{\xi - \xi_n}\right) - \frac{\prod_{n=1}^{M}(\xi + \xi_n)}{i(\xi - (\omega/V) - i\varepsilon)} \\ = \sigma^+(\xi, \omega) \prod_{n=1}^{M} (\xi + \xi_n) - \frac{\prod_{n=1}^{M}(\xi + \xi_n)}{i(\xi - (\omega/V) + i\varepsilon)}. \end{aligned} \tag{49}$$

By inspection we see that the left hand side is a function which is analytic in the lower half-plane and from (48) has at most a pole of order $M-1$ at infinity. Similarly, the right-hand side of (49) is analytic in the upper half-plane with at most a pole of order $M-1$ at infinity. (An estimate analogous to (48) holds for σ^+.) But from the equation itself, (49), these two analytic functions agree on the real axis and hence one is the analytic continuation of the other. It therefore follows from function theory that each side of (49) represents the same entire function having at most a pole of order $M-1$ at infinity. Analytically

$$p^-(\xi, \omega) \prod_{n=1}^{M} \left(\frac{\xi^2 - \lambda_n^2(\omega)}{\xi - \xi_n}\right) - \frac{\prod_{n=1}^{M}(\xi + \xi_n)}{i(\xi - (\omega/V) - i\varepsilon)} = \sum_{n=0}^{M-1} a_n(\omega)\xi^n, \tag{50}$$

where the undetermined coefficients a_n are functions of ω.

If we solve (50), then

$$p^-(\xi, \omega) = \prod_{n=1}^{M} \left(\frac{\xi - \xi_n}{\xi^2 - \lambda_n^2(\omega)}\right)\left[\sum_{n=0}^{M-1} a_n\xi^n + \frac{\prod_{n=1}^{M}(\xi + \xi_n)}{i(\xi - (\omega/V) - i\varepsilon)}\right]. \tag{51}$$

The expression in (51) has poles in the lower half-plane at $\xi = -\lambda_n(\omega)$, contrary to hypothesis. We therefore choose the a_n so that

$$\sum_{n=0}^{M-1} a_n(-\lambda_m)^n - \frac{\prod_{n=1}^{M}(\xi_n - \lambda_m)}{i(\lambda_m + (\omega/V))} = 0 \tag{52}$$

for $m = 1, \cdots, M$. (Note that ε has been set at zero in (52) since it no longer serves a useful purpose.) With the solution of the M linear equations (52) in the M unknowns a_n, the Wiener–Hopf procedure is complete. As will be seen in the following two sections, some remarkably simple forms result from this solution.

Before going on to more specific results, we mention an alternate method of solving (43). In view of the special form for K given by (18), (43) may be transformed into the differential equation

$$D(-\partial_x^2)\left\{p(x, \omega) - \exp\left[\frac{i\omega x}{V}\right]\right\} + S(\omega)N(-\partial_x^2)p(x, \omega) = 0.$$

A solution of this equation with unspecified boundary conditions is then substituted into (43) and the undetermined constants calculated. Although this approach is conceptually simple, the Wiener–Hopf method is far less cumbersome. Of course any valid method should lead to the same solution.

6. Response at the edge. To solve the linear system (52) we first place it in matrix form,

$$\mathcal{M}\mathbf{a} = \mathbf{f},$$

where

$$\mathcal{M}_{mn} = (-\lambda_m)^{n-1}, \qquad 1 \leqq m, n \leqq M,$$

$$\mathbf{a} = (a_0, a_1, \cdots, a_{M-1}),$$

$$f_m = \frac{\prod_{n=1}^{M}(\xi_n - \lambda_m)}{i((\omega/V)+\lambda_m)}.$$

We draw attention to two properties of the matrix, $\mathcal{M}$: (1) $\mathcal{M}$ is a Vandermonde matrix [19]; (2) each cofactor matrix of the last column of $\mathcal{M}$ is also a Vandermonde matrix. The determinant of a Vandermonde matrix has the form [19],

$$\det[\mathcal{M}] = \prod_{1 \leqq q < p \leqq M} (\lambda_q - \lambda_p). \tag{53}$$

Similarly, if we denote the cofactor matrix of $\mathcal{M}$ by $\mathcal{C}$ then the last column of $\mathcal{C}$ is given by

$$\mathcal{C}_{nM} = (-)^{n+M} \prod_{1 \leqq q < p \leqq M-1}' (\lambda_q - \lambda_p), \tag{54}$$

where the prime signifies that $p, q \neq n$. It then follows from (53), (54) and the form for a matrix inverse [17] that the last row of $\mathcal{M}^{-1}$ is given by

$$(\mathcal{M}^{-1})_{Mn} = \frac{1}{\prod_{1 \leqq q \leqq M}'(\lambda_q - \lambda_n)},$$

where the prime again indicates that the index $q \neq n$. This allows us to solve explicitly for the last component of $\mathbf{a}$,

$$a_{M-1} = \sum_{n=1}^{M} \frac{\prod_{m=1}^{M}(\xi_m - \lambda_n)}{i((\omega/V)+\lambda_n)\prod_{1 \leqq m \leqq M}'(\lambda_m - \lambda_n)}. \tag{55}$$

If in (50) we consider terms of $O(\xi^{M-1})$ for $|\xi| \uparrow \infty$, then with the aid of (48) we obtain

$$a_{M-1} = \frac{p_e(\omega)}{i} - \frac{1}{i},$$

which if inserted in (55) gives

$$p_e(\omega) = 1 + \sum_{n=1}^{M} \frac{\prod_{m=1}^{M}(\xi_m - \lambda_n)}{((\omega/V)+\lambda_n)\prod_{1 \leqq m \leqq M}'(\lambda_m - \lambda_n)}. \tag{56}$$

To further reduce this expression we make the following observation. If $P(z)$ is a monic of degree M in z with values $P(z_i)$ at the M distinct points z_i, $i = 1, \cdots, M$, then a simple interpolation formula is

$$P(z) = \prod_{m=1}^{M}(z - z_m) + \sum_{m=1}^{M} \frac{P(z_m)\prod_{n \neq m}(z - z_n)}{\prod_{n \neq m}(z_m - z_n)}$$

or if we divide by the first term of the right-hand side

$$\frac{P(z)}{\prod_{m=1}^{M}(z - z_m)} = 1 + \sum_{m=1}^{M} \frac{P(z_m)}{(z - z_m)\prod_{n \neq m}(z_m - z_n)}.$$

To compare this with (56) identify ω/V with z and z_n with $-\lambda_n$ and from this it follows that

$$p_e(\omega) = \prod_{n=1}^{M} \frac{(\omega/V)+\xi_n}{(\omega/V)+\lambda_n}. \tag{57}$$

Comparison of (57) with $p_f(\omega)$, (37), shows that this may be written

$$p_e(\omega) = p_f(\omega) \prod_{n=1}^{M} \frac{(\omega/V)-\lambda_n}{(\omega/V)-\xi_n}. \tag{58}$$

Causality. The temporal response at the origin due to the stimulus $\tilde{e}$, (33), is given by

$$\rho_e(t) = \frac{1}{2\pi}\int_{-\infty}^{\infty} \exp[i\omega t]\tilde{e}(\omega) \prod_{n=1}^{M} \frac{(\omega/V)+\xi_n}{(\omega/V)+\lambda_n(\omega)}\, d\omega. \tag{59}$$

This solution should be causal. In particular, any stimulus arriving at the edge from the dark side of the eye ($V \leqq 0$) should not elicit a response before its arrival. (If $V \geqq 0$, an anticipatory "Mach band" response occurs, see § 8.) To demonstrate causality it is sufficient to show that the denominator in (59) $\prod_{n=1}^{M}((\omega/V)+\lambda_n(\omega))$ has neither zeros nor branch points in the lower half-plane. In § 3 it was shown that this product has no branch points in the lower half-plane. Furthermore, $\operatorname{Im}[\lambda_n(\omega)] > 0$, (25), therefore, for $V < 0$ and ω in the lower half-plane $\operatorname{Im}((\omega/V)+\lambda_n) > 0$ and we have proven our assertion.

7. Response in neighborhood of edge. We return to (51) and rewrite it in the form

$$p^{-}(\xi,\omega) = \frac{1}{(\xi-(\omega/V)-i\varepsilon)} \prod_{n=1}^{M}\left(\frac{\xi-\xi_n}{\xi-\lambda_n}\right)\left[\frac{i(\xi-(\omega/V))\sum_{n=0}^{M-1} a_n\xi^n + \prod_{n=1}^{M}(\xi+\xi_n)}{i\prod_{n=1}^{M}(\xi+\lambda_n)}\right].$$

From the construction given in the previous section, the denominator exactly divides the numerator in the bracketed expression. The result of this division is $(a_{M-1}-i)$, which from the previous section (see (55) and below) is $-ip_e(\omega)$. If this is substituted into (51) then

$$p(\xi,\omega) = \frac{p_e(\omega)}{i(\xi-(\omega/V)-i\varepsilon)} \prod_{n=1}^{M} \frac{(\xi-\xi_n)}{(\xi-\lambda_n(\omega))}. \tag{60}$$

(Note that the minus sign superscript has been omitted from p in (60) since it is no longer necessary.)

The spatial inversion of (60) is given by

$$p(x,\omega) = \frac{1}{2\pi i}\int_{-\infty}^{\infty} \frac{1}{(\xi-(\omega/V)-i\varepsilon)} \prod_{n=1}^{M}\left(\frac{\xi-\xi_n}{\xi-\lambda_n}\right) \exp(i\xi x)\, d\xi\, p_e(\omega). \tag{61}$$

Since the poles of the integrand of (61) all lie in the upper half-plane $p(x,\omega)$ vanishes for $x < 0$, as it should.

If we evaluate (61) by closing the contour in the upper half-plane we find

$$p(x,\omega) = p_e(\omega)\left\{\prod_{n=1}^{M}\left(\frac{(\omega/V)-\xi_n}{(\omega/V)-\lambda_n}\right)\exp\left[i\frac{\omega}{V}x\right] - \sum_{m=1}^{M} \frac{\prod_{n=1}^{M}(\lambda_m-\xi_n)}{((\omega/V)-\lambda_m)\prod_n'(\lambda_m-\lambda_n)}\exp[i\lambda_m x]\right\}.$$

If (58) is substituted,

$$(62)\quad p(x,\omega)=p_f(\omega)\exp\left[\frac{i\omega x}{V}\right]-p_e(\omega)\sum_{m=1}^{M}\frac{\prod_{n=1}^{M}(\lambda_m-\xi_n)}{((\omega/V)-\lambda_m)\prod_n'(\lambda_m-\lambda_n)}\exp[i\lambda_m x].$$

The interpolation formula also yields the identity

$$\prod_{n=1}^{M}\left(\frac{(\omega/V)-\xi_n}{(\omega/V)-\lambda_n}\right)-\sum_{m=1}^{M}\frac{\prod_{n=1}^{M}(\lambda_m-\xi_n)}{((\omega/V)-\lambda_m)\prod_n'(\lambda_m-\lambda_n)}=1$$

which when substituted into (58) and then into (62) yields

$$(63)\quad \begin{aligned} p(x,\omega)&=p_e(\omega)\exp\left[\frac{i\omega x}{V}\right]\\ &\quad -p_e(\omega)\sum_{m=1}^{M}\frac{\prod_{n=1}^{M}(\lambda_m-\xi_n)}{((\omega/V)-\lambda_m)\prod_n'(\lambda_m-\lambda_n)}\left\{\exp[i\lambda_m x]-\exp\left[\frac{i\omega x}{V}\right]\right\}.\end{aligned}$$

From (62) we see that in the limit of $x\uparrow\infty$, $p(x,\omega)$ goes to the full eye result (37), while from (63) it goes to the edge result for $x\downarrow 0$.

The analysis which has been presented thus far is based in part on the form, (18), for $K(\xi)$. As mentioned at the time of its introduction this form is appropriate for a kernel, $K(x)$, which is made up of a sum of back-to-back exponentials. However, even under more general circumstances a transformed kernel, $K(\xi)$, possesses a finite approximation of the form (18), see [20]. In addition, our results also can apply in the limit $M\uparrow\infty$ if the products in (18) converge. This, for example, is the case if $K(\xi)$ is a meromorphic function of low enough order, [21].

8. Illustrations and discussion. Under laboratory conditions the various operators appearing in (5) are fit by models which incorporate an understanding of the underlying mechanisms and, as well, a suitable number of parameters so as to achieve a close fit with recorded data. The resulting forms take on a complicated structure [4], and as a result, machine calculations are required. For purposes of exposition we illustrate the preceding theory with a model which only seeks to capture the qualitative features of an accurate model. (At the close of this section we briefly discuss more accurate models and a comparison with experiment.)

We choose

$$(64)\qquad K(x)=\tfrac{1}{2}\exp[-|x|]$$

and

$$(65)\qquad S(t)=S_0H(t)\exp[-t]$$

with the corresponding transforms given by

$$(66)\qquad K(\xi)=\frac{1}{(\xi+i)(\xi-i)}$$

and

$$(67)\qquad S(\omega)=\frac{S_0}{1+i\omega}.$$

Note, the absence of scales in (64)–(67) signifies that distance is normalized by the spatial scale of inhibition and time by the temporal scale of S.

Infinite eye. For later purposes it is useful to consider first some elementary cases.

The purely temporal problem has the solution (6), which also may be written in the form

$$\rho(t) = p * e(t).$$

In the present instance we find

$$p = \delta(t) - S_0 H(t) \exp[-(1+S_0)t]. \tag{68}$$

The solution operator, p, itself has the interpretation of being the response to a delta function stimulus. In addition to the resulting delta function of excitation, this stimulus produces an inhibitory rebound in the form of a decaying exponential with strength S_0 and time-scale $(1+S_0)^{-1}$.

Another elementary case is that of purely spatial response,

$$\rho(x) = e(x) - S_0 \int_{-\infty}^{\infty} K(x-y)\rho(y)\, dy.$$

In this case if we write

$$\rho = \int_{-\infty}^{\infty} p(x-x_0)e(x_0)\, dx_0 = p * e,$$

then it easily follows that

$$p = \delta(x-x_0) - \frac{S_0}{2\alpha} \exp(-\alpha|x-x_0|), \tag{69}$$

where

$$\alpha = \sqrt{1+S_0}.$$

Thus a delta function stimulus produces a delta function excitation and a symmetric inhibitory skirt of scale $1/\alpha$, and which has the indicated strength.

Next we turn to the case of a drifting pattern. If (66) and (67) are substituted into (37) we obtain

$$p_f(\omega) = \frac{(\omega^2/V^2)+1}{(\omega^2/V^2)+1+(S_0/(1+i\omega))} = 1 - \frac{S_0}{(1+i\omega)[(\omega^2/V^2)+1+(S_0/(1+i\omega))]}.$$

The inverse transform of the first term at the right is the "delta function," $\delta(t)$. To perform the inversion on the second term we set $z = i\omega$ to obtain

$$p_f(t) = \delta(t) + \frac{S_0 V^2}{2\pi i} \int_{-i\infty}^{i\infty} \frac{\exp(zt)\, dz}{(z-z_0)(z-z_1)(z-z_2)}, \tag{70}$$

with a path of integration along the imaginary axis. V, the speed, can be expressed parametrically by

$$V^2 = \frac{z_0^3 + z_0^2}{z_0 + 1 + S_0}, \qquad 0 \leqq z_0 \leqq \infty, \tag{71}$$

in terms of which the additional roots are

$$z_{1,2} = \frac{1+z_0}{2}\left\{-1 \pm \sqrt{1 - \frac{4z_0(1+S_0)}{(1+z_0)(z_0+1+S_0)}}\right\}. \tag{72}$$

The roots z_1, z_2 lie in the left half-plane, and are either both real or complex conjugates.

If we carry out the integration in (70) then

$$p_f(t)=\delta(t)-S_0V^2\left\{\frac{H(-t)\exp(z_0t)}{(z_0-z_1)(z_0-z_2)}-\frac{H(t)}{z_1-z_2}\left(\frac{\exp(z_1t)}{z_1-z_0}-\frac{\exp(z_2t)}{z_2-z_0}\right)\right\}. \tag{73}$$

The first column of Fig. 2 contains plots of (73) for a variety of values of V. Under the low speed limit $|V|\downarrow 0$, (73) has the asymptotic form

$$p_f\sim\delta(t)-\frac{S_0|V|}{2\alpha}\exp[-\alpha|V|t]. \tag{74}$$

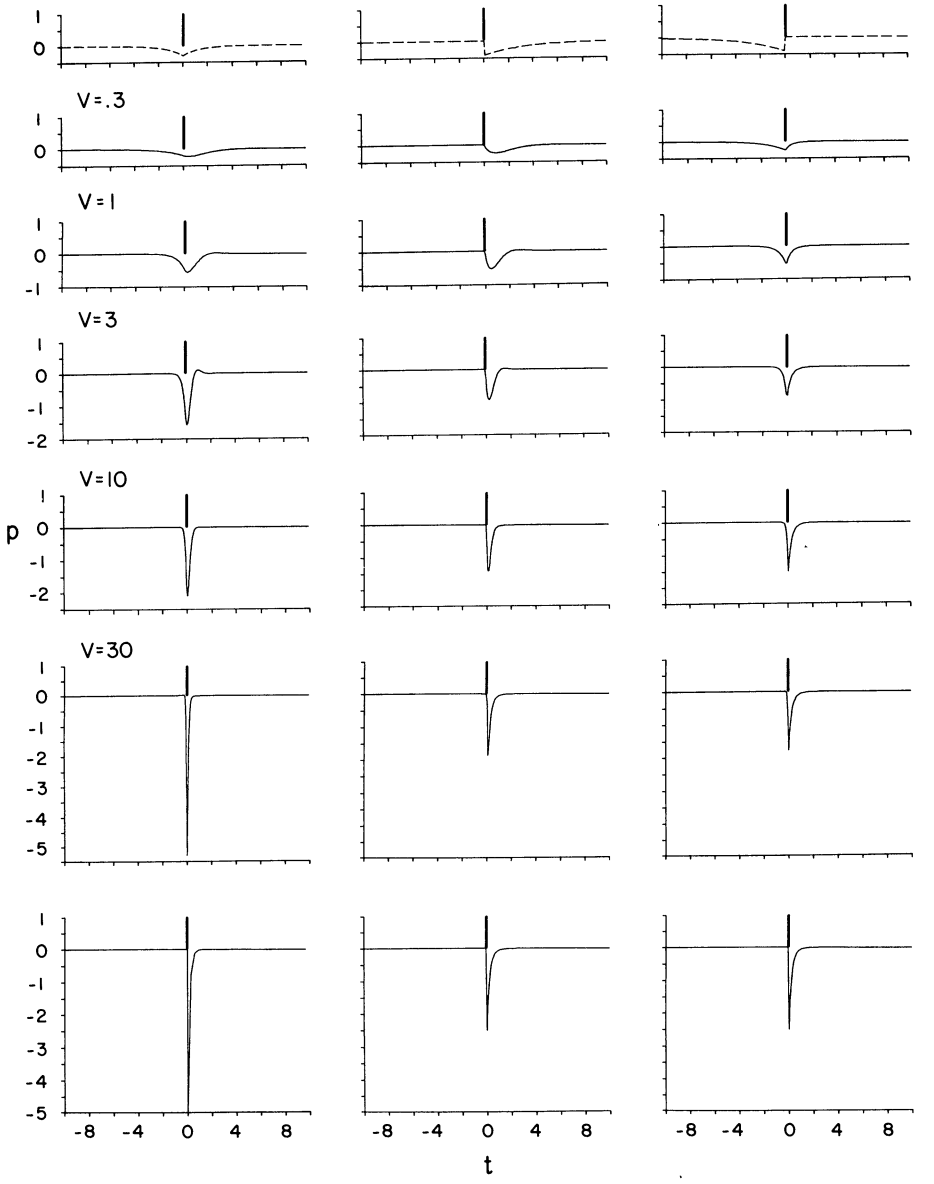

FIG. 2. *Model responses for a moving delta function stimulus based on the simplified case,* (64) *and* (65). *First column, full eye records; second column, half eye records with stimulus coming out of the dark; third column, half eye records with stimulus coming out of the light. Successive rows show responses at increasing speeds. The first row is based on the quasi-stationary hypothesis, see* (74), *at the value* $V = .3$ *and the last row on the purely temporal response,* (68).

The top figure, dashed line, is the graph of (74) for $V = .3$, while the second plot is of (73) at the same speed. In each figure the delta function is indicated by a heavy vertical line segment. Comparison of (74), which is symmetrical in time, with (69) yields the plausible interpretation of its being the response due to a quasi-stationary point source. Under this interpretation the source position, x_0, in (69) is permitted to translate (slowly) with velocity, V, i.e., we write $x_0 = Vt$ in (69). (On dimensional grounds we must also multiply (69) by $|V|$.) Thus in the low speed limit a point stimulus is preceded by an inhibitory skirt, known as a Mach band [22], and followed by an almost symmetrically placed skirt of inhibition. In contrast with the anticipatory Mach band, which is due to the passive spread of inhibition, the trailing "skirt" contains in addition the temporal inhibitory rebound which we saw in (68) follows the excitation.

As the speed increases the asymmetry becomes more pronounced, and at unbounded speeds the anticipatory Mach band vanishes entirely. Under this limit the delta function arrives before the passive spread can be established. We note that the asymptotic form of (73) for $|V| \uparrow \infty$ is just (68), the purely temporal response. This is also plausible, for in this case the entire neighborhood of a receptor receives the delta function stimulus at the same time, thereby duplicating the conditions of the purely temporal problem. It also follows that the deep inhibitory trough at high speeds is due to the synchronized inhibitory arrivals by the entire neighborhood of a point.

At intermediate speeds, notably at $V = 3$, we observe an excitatory rebound. This effect can be regarded as the response at a point when the inhibitory lobe moves into the neighborhood of that point. It is noticeable only at intermediate speeds when it is not dominated by other effects. An inspection of the numerical form of (73) actually shows damped oscillations extending to infinity.

Semi-infinite eye. We again start with a somewhat elementary case, namely that of a steady illumination pattern falling on a semi-infinite eye. In this case the equation to be solved is

$$\rho(x) = e(x) - S_0 \int_0^\infty K(x-y)\rho(y)\, dy,$$

and the method of solution is subsumed by the Wiener–Hopf analysis given earlier. In particular if we consider the fundamental solution

$$p(x, x_0) = \delta(x-x_0) - S_0 \int_0^\infty K(x-y)p(y, x_0)\, dy$$

which has the property

$$\rho = \int_{-\infty}^\infty p(x; x_0)e(x_0)\, dx_0,$$

then we find

$$p = \delta(x-x_0) - \frac{S_0}{2\alpha}\left[\frac{\alpha-1}{\alpha+1}\exp(-\alpha(x+x_0)) + \exp(-\alpha|x-x_0|)\right] \tag{75}$$

for $x, x_0 \geqq 0$.

With the exception of the first term of the bracket this is the same as the result for the infinite eye given by (69). For $x_0 \uparrow \infty$ this solution, (75), approaches (69).

Next we consider the case of a drifting pattern. For the special case under study (59) yields

$$p_e(t) = \frac{1}{2\pi}\int_{-\infty}^\infty \frac{((\omega/V)+i)\exp[i\omega t]}{(\omega/V)+i\sqrt{1+S_0/(1+i\omega)}}\, d\omega,$$

which if we set $z = i\omega$ yields

$$p_e(t) = \frac{1}{2\pi i}\int_{-i\infty}^{i\infty} \frac{((z/V)-1)\exp[zt]\,dt}{(z/V)-w(z)}, \tag{76}$$

where

$$w(z) = \sqrt{\frac{z+1+S_0}{z+1}}. \tag{77}$$

In order to evaluate this integral we decompose the integrand as follows

$$\frac{(z/V)-1}{(z/V)-w(z)} = 1 + \sum_{n=0}^{2} \frac{B_n}{z-z_n} + V\sum_{n=0}^{2} \frac{B_n}{z-z_n}\frac{w(z)}{z_n}, \tag{78}$$

where

$$B_n = \frac{z_n(z_n - V)(z_n+1)}{\prod_{j\neq n}(z_n - z_j)}$$

and z_n, $n = 0, 1, 2$ are the roots indicated in (71) and (72).

The inversion of the first two terms is direct,

$$\frac{1}{2\pi i}\int_{-i\infty}^{i\infty}\left(1+\sum_{n=0}^{2}\frac{B_n}{z-z_n}\right)\exp(zt)\,dz$$

$$= \delta(t) - H(-t)B_0\exp(z_0t) + H(t)\{B_1\exp(z_1t) + B_2\exp(z_2t)\}.$$

In this we have used the fact that Re $z_0 > 0$, Re $z_{1,2} < 0$. The remaining sum in (78) can be evaluated in terms of the following formula,

$$\mathcal{J}_k(t) = \frac{1}{2\pi i}\int_B \frac{\exp(zt)}{z-z_k}\sqrt{\frac{z+1+S_0}{z+1}}\,dz$$

$$= H(t)\exp(z_kt)\left\{I_0\left(\frac{S_0t}{2}\right)\exp\left[-\left(1+z_k+\frac{S_0}{2}\right)\right] + (1+S_0+z_k)\right. \tag{79}$$

$$\left.\cdot\int_0^t I_0\left(\frac{S_0u}{2}\right)\exp\left[-\left(1+z_k+\frac{S_0}{2}\right)u\right]du\right\},$$

where I_0 is the modified Bessel function [23]. This is based on a Laplace inversion (Erdélyi [24, formula 27, p. 235]) and as a result the path of integration, denoted by B, must lie to the right of all singularities of the integrand of $\mathcal{J}_k$. With the exception of the pole at $z = z_0$ this is true of the terms of (78). Therefore with this additional pole contribution in mind we find

$$\frac{1}{2\pi i}\int_{-i\infty}^{i\infty}\exp(zt)\sum_{n=0}^{2}\frac{B_n}{z_n}\frac{w(z)}{z-z_n}\,dz = -B_0\exp(z_0t)\frac{w(z_0)}{z_0} + \sum_{n=0}^{2}\frac{B_n}{z_n}\mathcal{J}_n(t).$$

After some rearrangement of terms this leads to

$$p_e(t) = \delta(t) - B_0(1+\operatorname{sgn} V)H(-t)\exp(z_0t) + H(t)\sum_{n=1}^{2}B_n\exp(z_nt)$$

$$-H(t)(\operatorname{sgn} V)\exp(z_0t) + H(t)V\sum_{n=0}^{2}\frac{B_n}{z_n}\mathcal{J}_n(t). \tag{80}$$

In deriving this we have used

$$w(z_0)=\frac{z_0}{|V|}$$

which follows from (71) and (77). It should be noted that the coefficient of $H(-t)$ vanishes for $V<0$, so that causality is preserved.

The asymptotic expansion of p_e for $|V|$ large is given by the following:

$$p_e \sim \delta(t)-H(t)\frac{S_0}{2}\exp\left[-\left(1+\frac{S_0}{2}\right)t\right]\left(I_0\left(\frac{S_0 t}{2}\right)-I_1\left(\frac{S_0 t}{2}\right)\right), \qquad |V|\uparrow\infty. \tag{81}$$

Columns 2 and 3 of Fig. 2 contain plots of the response at the edge of a half infinite eye. The second column describes the response when a point stimulus moves across the edge from the left (out of the dark) while the third column gives the analogous description when the point stimulus crosses the edge from the right (out of the light). A number of features are worth noting. The last two entries of the last row, $|V|\uparrow\infty$, are identical and are taken from the asymptotic formula (81). Note that the maximum inhibition is half that of the infinite case, (68), as might be expected since inhibition is being received from only half the receptors. (Less expected perhaps is the fact that the time course is functionally different in the half and full eye cases, (68) and (81).)

In keeping with the requirement of causality, each response in the second column is zero before the stimulus reaches the edge. The inhibition then builds up to a maximum as more receptors are excited by the passing source stimulus. At high speeds the inhibition is deep and is reached quickly, while at low speeds it is shallow and reached after longer times. At intermediate speeds, see especially, $V=-3$, there is an excitatory rebound as in the infinite eye case, and it occurs for the same reason.

The response curves in the third column have anticipatory Mach bands for the same reasons given in the case of an infinite eye. In contrast with the infinite eye case however, the peak inhibition occurs at the moment the source crosses the edge. For the infinite eye the inhibition continues to build up after the source crosses and the maximum occurs later. For the half eye we see that the inhibition rapidly goes to zero after the source passes the edge. In this case there no longer is an inhibitory contribution when the source is on the dark side of the edge.

The last two entries of the first row, dashed curves, indicate the time courses which are predicted from the quasi-stationary hypothesis applied to (75). As before, this entails using the steady half-space solution, (75), to predict the response to a drifting pattern under the assumption $x_0=Vt$. Unlike the situation for the infinite eye, this is now incorrect as the figure indicates. A low speed asymptotic expansion of (80) is not given here since it results in only minor simplification. In any event it bears no resemblance to (75).

Comparison with experiment. The model just discussed lacks many of the detailed features of the theoretical model used for comparison with experiment, [4]. In addition to more complex forms for the inhibitory kernel, K, and the lateral inhibitory encoding, S, one must also consider the sequence of transductions which enter into the definition of the effective illumination (9), and which we have been able to ignore in our analytical investigation. The result of these considerations is given elsewhere [4] but for completeness of exposition we briefly discuss some of these results.

The experimental stimulus consisted of a uniformly drifting light pattern made up of a step-function followed by an exponential fall-off. The response of a neuron to this stimulus was measured and the results averaged over a large number of presentations.

The responses in dimensional units for the indicated speed (not to be compared with our normalized speed) are shown on the second row of Fig. 3. The first record is for the full eye, the next for the half eye shows the response for the stimulus coming out of the dark, and the last for the half eye and stimulus coming out of the light. Above these is shown the comparable theoretical predictions which follow from the analysis presented in this paper but using a more elaborate model. We note that the agreement is good. Next we comment on some of the features of these records.

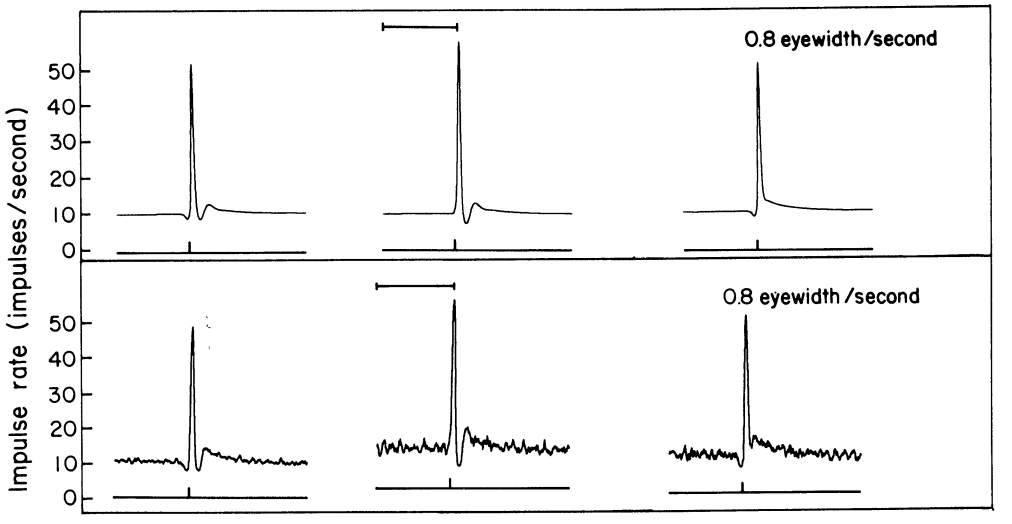

FIG. 3. *Typical experimental and theoretical records taken from* [4]. *The second row contains averaged experimental records taken at a speed of .8 eyewidths/sec. The first row follows computations based on the theory of this paper. The three columns follow the convention in Fig. 2. The scale markers indicate a two second interval and the tic marks the passage time of the step.*

With regard to the full eye records we observe the presence of an anticipatory "Mach band", a sharp response when the light step crosses (indicated by a tic mark), and an equally sharp reduction in the impulse rate due in part to self-inhibition (not discussed here but included in E) and in part from the sudden rise in inhibition from the neighboring receptors which are at peak response. The reason for the excitatory rebound was explained in our discussion of the model. Turning to the "out of the dark" case we again see the abrupt rise (to a higher peak than the full eye case) without an anticipatory "Mach band" as is required by causality, followed by features found in the full eye case. Finally the feature to note in the "out of the light" record is the absence of an inhibitory notch since there is now no highly responsive neighbor to inhibit the test receptor.

Acknowledgments. It is with pleasure that I express deep gratitude to Bruce Knight, who was generous with his time and ideas. I also thank Floyd Ratliff for his encouragement and for arousing my interest in this problem. Thanks are also due to Scott Brodie for his helpful criticism in the preparation of this manuscript, and to Mark Kac for pointing out the connection with differential equations mentioned at the close of § 5.

The author is also grateful to the John Simon Guggenheim Memorial Foundation for their fellowship support during the course of this work.

REFERENCES

[1] R. B. BARLOW, JR., *Inhibitory fields in the Limulus lateral eye*, J. Gen. Physiol., 54 (1969), pp. 383–396.

[2] S. E. BRODIE, B. W. KNIGHT AND F. RATLIFF, *The response of the Limulus retina to a moving stimulus: A prediction by Fourier synthesis*, J. Gen. Physiol., 72 (1978), pp. 129–166.

[3] ———, *The spatiotemporal transfer function of Limulus lateral eye*, J. Gen. Physiol., 72 (1978), pp. 167–202.

[4] L. SIROVICH, S. E. BRODIE AND B. W. KNIGHT, *The effect of boundaries on the response of a neural network*, Biophys. J., 28 (1979), pp. 423–446.

[5] H. K. HARTLINE AND F. RATLIFF, *Inhibitory interaction of receptor units in the eye of Limulus*, J. Gen. Physiol., 10 (1957), pp. 357–376.

[6] B. W. KNIGHT, J. TOYODA AND F. A. DODGE, *A quantitative description of the dynamics of excitation and inhibition in the eye of Limulus*, J. Gen. Physiol., 56 (1970), pp. 421–437.

[7] G. D. LANGE, *Dynamics of inhibitory interactions in the eye of Limulus: experimental and theoretical studies*, Ph.D. thesis, The Rockefeller Institute, New York, 1965.

[8] R. B. BARLOW, JR. AND G. D. LANGE, *A nonlinearity in the inhibitory interactions in the lateral eye of Limulus*, J. Gen. Physiol., 63 (1974), pp. 579–589.

[9] R. B. BARLOW, JR. AND D. A. QUARLES, *Mach bands in the lateral eye of Limulus: Comparison of theory and experiment*, J. Gen. Physiol., 65 (1975), pp. 709–730.

[10] K. KIRSCHFELD AND W. REICHARDT, *Die Verarbeitung stationarer optischer Nachrichten im Komplexauge von Limulus, (Ommatidien-Sehfeld und Verteilung der Inhibition)*, Kybernetik, 2 (1964), pp. 43–61.

[11] F. A. DODGE, *Inhibition and excitation in the Limulus eye*, Processing of Optical Data by Organisms and by Machines, Proc. of the International School of Physics "Enrico Fermi," Course XLIII, W. Reichardt ed., Academic Press, New York, 1969, pp. 341–365.

[12] F. RATLIFF, B. W. KNIGHT, F. A. DODGE AND H. K. HARTLINE, *Fourier analysis of dynamics of excitation and inhibition in the eye of Limulus: Amplitude, phase, and distance*, Vision Res., 14 (1974), pp. 1155–1168.

[13] F. RATLIFF, ed., *Studies on Excitation and Inhibition in the Retina*, The Rockefeller University Press, 1974.

[14] R. B. BARLOW, JR., *Inhibitory fields in the Limulus lateral eye*, Ph.D. thesis, The Rockefeller University, New York, 1967.

[15] D. JOHNSTON AND H. WACHTEL, *Electrophysiological basis for the spatial dependence of the inhibitory coupling in the Limulus retina*, J. Gen. Physiol., 67 (1976), pp. 1–25.

[16] B. W. KNIGHT, *The horseshoe crab: A little nervous system that is solvable*, Lectures on Mathematics in the Life Sciences, vol. 4, J. B. Cowan, ed., American Mathematical Society, Providence, RI, 1973.

[17] B. NOBLE, *The Wiener-Hopf Technique*, Pergamon Press, New York, 1958.

[18] L. SIROVICH, *Techniques of Asymptotic Analysis*, Springer-Verlag, New York, 1971.

[19] S. PERLIS, *Theory of Matrices*, Addison-Wesley, Cambridge, MA 1952.

[20] V. I. SMIRNOV AND N. A. LEBEDEV, *Functions of a Complex Variable*, M.I.T. Press, Cambridge, MA, 1968.

[21] E. C. TITCHMARSH, *The Theory of Functions*, Oxford University Press, London, 1950.

[22] F. RATLIFF, *Mach Bands: Quantitative Studies on Neural Networks in the Retina*, Holden-Day, San Francisco, 1965.

[23] M. ABRAMOWITZ AND I. A. STEGUN, eds., *Handbook of Mathematical Functions*, National Bureau of Standards AMS 55, U.S. Gov. Printing Office, Washington, DC, 1965.

[24] A. ERDÉLYI, ed., *Table of Integral Transforms, Bateman Project*, Vol. 1, McGraw-Hill, New York, 1954.